

Design and Performance of an Inductive Current Probe for Integration Into the Trace Suspension Assembly

Anthony B. Kos, Thomas J. Silva, Pavel Kabos, Matthew R. Pufall, Donald C. DeGroot, Larry Webb, and Marc Even

Abstract—A low-cost, inductive current probe designed for integration into a disk drive trace suspension assembly is described. The main consideration for this design was to use the same materials currently found in trace suspension assemblies, and thus reducing costs, while at the same time providing a drive characterization tool capable of measuring 100 ps head field rise times. The inductive current probe consists of a pair of differential copper conductors fabricated adjacent to the write driver interconnects and magnetically coupled via a Ni-Fe thin film placed on top of these conductors. The differential conductor pair is connected to a high-speed sampling oscilloscope to measure the speed of the write current pulse and thus infer the write head field rise time. Data are shown for high-speed pulses generated with rise times of less than 100 ps.

Index Terms—Current probe, head field rise time, inductive voltage, trace suspension assembly, write head current.

I. INTRODUCTION

IN THE design of high-data-rate disk drives, it is instructive to know the rise time of the write head current pulse. Externally inserted current probes have been used under laboratory conditions to measure write head current waveforms and infer field rise times [1]. However, it would be useful to be able to measure actual current waveforms in a commercial drive or prototype device under normal operating conditions using the existing interconnects. We present an inductive current probe as a tool for accomplishing this goal while perturbing the drive signals as little as possible.

The costs associated with this method are low, since conventional trace suspension materials and manufacturing techniques are used to fabricate the current probe. This is of some advantage, since the current probe could even be present on every assembly manufactured for use in quality assurance. In addition, since the probe pickup is incorporated between the highly overdriven write drivers (required to provide short head field rise times [2]) and the thin film write head, this is a true *in-situ* current rise time measurement.

Manuscript received June 25, 2001.

A. B. Kos, T. J. Silva, P. Kabos, and M. R. Pufall are with the National Institute of Standards and Technology, Magnetic Technology Division, Boulder, CO 80305 USA (e-mail: kos@boulder.nist.gov).

D. C. DeGroot is with the National Institute of Standards and Technology, Radio Frequency Technology Division, Boulder, CO 80305 USA (e-mail: degroot@boulder.nist.gov).

L. Webb and M. Even are with Hutchinson Technology, Hutchinson, MN 55350 USA (e-mail: larry.webb@hti.htch.com).

Publisher Item Identifier S 0018-9464(02)01288-8.

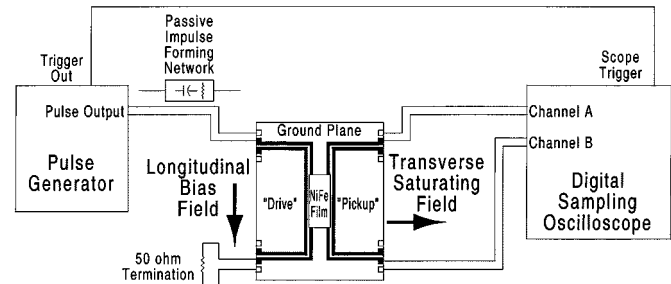


Fig. 1. System diagram for inductive current probe. The arrows indicate the direction that the longitudinal bias and transverse saturating fields are applied. To perform an impulse response measurement, the passive impulse-forming network shown is inserted into the output path of the pulse generator where indicated.

The inductive current probe (Fig. 1) consists of two sets of differential copper conductors over a dielectric-covered, stainless steel ground plane, which are magnetically coupled via a Ni-Fe thin film placed upside-down onto the conductors. Since the Ni-Fe film is not actually part of the trace suspension fabrication process, the process does not need to be modified to include Ni-Fe thin film production. The copper conductors are coated with a layer of polyimide, approximately 1 μm thick, to prevent the Ni-Fe film from shorting to the conductors. In an actual drive, the first set of conductors would be the write driver interconnects integrated into the trace suspension assembly. The other set, used for signal pickup, is connected via microwave probes to a high-bandwidth digital sampling oscilloscope.

To test the design and performance of the current probe, a commercially available, broadband step generator is connected with a single-ended connection via the ground plane to the inner conductor on the drive side. The other end is terminated in 50 ohms. This pulse generator is capable of delivering 10 V steps with 50 ps rise times and 10 ns duration, to simulate very fast write current pulses. Each end of the inner conductors on the pickup side is connected, in a single-ended fashion, to the two channels of a digital sampling oscilloscope. This sampling oscilloscope, which has the 14-bit dynamic range necessary to extract millivolt-level signals, averages the waveforms more than 500 times to achieve the required signal-to-noise ratio (SNR). The signals present on the two oscilloscope channels are differentially detected, thus removing capacitively coupled signals that are common to both channels. Two measurements, one with the Ni-Fe film saturated and one with the film left free to rotate, are taken and subtracted to yield a result independent of background signals. This subtraction process is very important to the measurement; it removes

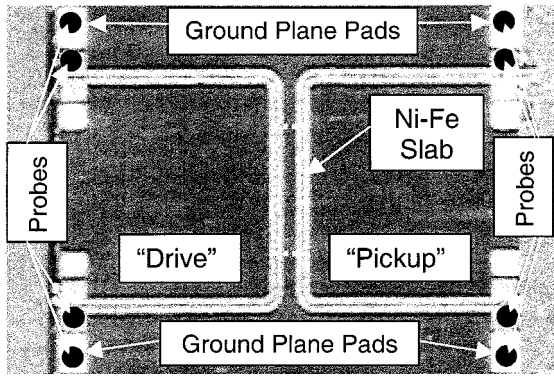


Fig. 2. Photograph of inductive current probe test structure. The Ni-Fe thin film is placed upside-down onto the conductors and located in the center of the test structure as indicated in Fig. 1. High-bandwidth (40 GHz) microwave probes are used to make contact to the ground plane and copper conductors seen at the edges of the photograph. Inner conductor spacing shown is $300 \mu\text{m}$.

all background signals, inductive or capacitive, that do not magnetically propagate through the Ni-Fe film. The results of the subtraction are integrated to yield the response of the magnetic system to the applied current pulse.

An additional set of measurements is required to obtain the impulse response of the current probe assembly. A passive impulse-forming network is attached to the previously mentioned fast pulse generator in order to generate a 1 V impulse whose full width at half maximum is less than 100 ps. This set of measurements yields the impulse response of the magnetic system. The actual step current waveform can be obtained once the previously obtained response to the pulse current is deconvolved with the measured impulse response.

II. DESIGN OF INDUCTIVE CURRENT PROBE

A. Trace Suspension Fabrication

Conventional trace suspension material is supplied in sheet form consisting of a thin, $18 \mu\text{m}$ copper layer separated from a $20 \mu\text{m}$ stainless steel ground plane by a layer of polyimide, $18 \mu\text{m}$ thick. Standard photolithographic techniques are used for patterning of the copper traces followed by chemical etching. Access to the stainless steel ground plane is provided by mechanically removing the polyimide wherever contact is required, leaving a contact window for the microwave probe contacts. A photograph of a typical test structure is seen in Fig. 2. The copper conductors are $100 \mu\text{m}$ wide and the center overlapping section where the Ni-Fe film is laid is about 4.5 mm long. The spacing between the inner drive conductors and the inner pickup conductors, defined from conductor inner edge to conductor inner edge, was varied from $50 \mu\text{m}$ to $500 \mu\text{m}$ in $50 \mu\text{m}$ increments. This parallel microstrip geometry is patterned to resemble the write driver interconnects in a typical trace suspension assembly. Each microstrip line is designed, using microwave finite-element modeling, to have a nominal characteristic impedance of 50 ohms and a differential impedance of 100 ohms. For the purpose of evaluating the usefulness of the inductive current probe, only the innermost conductors are used; the outermost conductors are left unconnected and are not used at all in this work.

B. Ni-Fe Film

Ni-Fe (81% Ni, 19% Fe) films, 200 nm thick, were grown by DC magnetron sputtering in the presence of a 16 kA/m (200 Oe) magnetic field onto glass cover slides. The glass cover slides were chosen to prevent eddy current effects in the substrate material from affecting the measurement results. The films were measured on a conventional induction-field (B - H) loop to determine their magnetic properties. The square loops thus obtained had a coercivity of roughly 100 A/m (1.2 Oe) and a saturation magnetization of 800 kA/m. The anisotropy induced by deposition in field is about 400 A/m (5 Oe).

III. THEORY

A. General

For a magnetic thin film sample placed directly on top of the $100 \mu\text{m}$ wide copper conductor, we would expect a pulsed field of approximately 1000 A/m (12.5 Oe) from $H_P = I/2w$, derived for fields above a uniform current sheet, where w is the width of the sheet carrying current I ($I \approx 200 \text{ mA}$ for a 10 V pulse driven into 50 ohms). Since the film is separated from the conductors by a $1 \mu\text{m}$ layer of polyimide, the actual pulsed field seen by the film will be slightly smaller. If the magnetic film is placed such that the anisotropy axis is perpendicular to the direction of the pulsed field, the magnetization of the film will rotate and propagate to the pickup side, and this action will induce a voltage V_P across the pickup conductors. For sufficiently small rotations, linear system theory can be applied to the analysis of the resulting voltage waveforms. An externally generated DC bias field, H_B , applied parallel to the anisotropy axis, can be used to “stiffen” the magnetization, and thus force a response with greater linearity, but at the expense of induced signal amplitude. Measurements taken over a range of applied bias fields reveal that $H_B = 0$ is adequate for our purposes, indicating that the Ni-Fe samples used have a well-established, predominately single-domain anisotropy axis. This also makes the inductive probe technique more easily applied to actual hard drive measurements, since only the saturating field need be applied.

The induced voltage obtained above, $V_P = -d\Phi/dt$, is related to the average magnetization perpendicular to the anisotropy axis, M_y , by [3]

$$\overline{M}_y = \frac{4}{\mu_0 \delta l \epsilon} \int V_P dt \quad (1)$$

where δ is the film thickness, l is the film length and ϵ is the coupling efficiency between the magnetic film and the pickup line.

Consider the static one-dimensional micromagnetic calculation of an average magnetization distribution in equilibrium as shown in Fig. 3. Integrating M over the length of the pickup line to obtain the transmitted flux gives the DC coupling efficiency ϵ , which is defined as the detected flux on the pickup side normalized with respect to the flux integrated over the drive side. Fig. 4 shows the coupling efficiency for inner conductor edge to inner conductor edge distances of $50 \mu\text{m}$, $100 \mu\text{m}$, $200 \mu\text{m}$, $250 \mu\text{m}$, and $300 \mu\text{m}$. While such a calculation ignores the important details of dynamic effects within the magnetic film, we

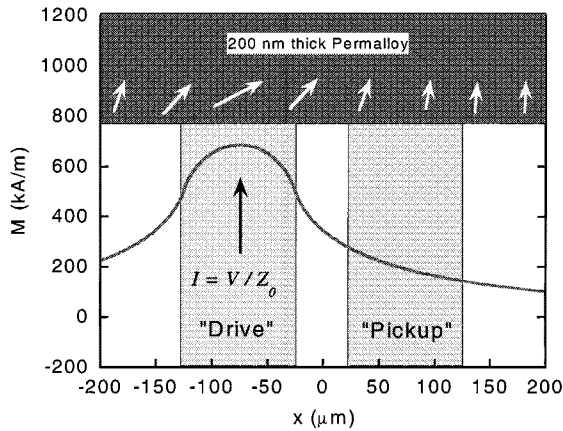


Fig. 3. One-dimensional micromagnetic simulation. The coupling efficiency calculated by the micromagnetic simulation, for the 50 μm conductor spacing shown, is approximately 31%.

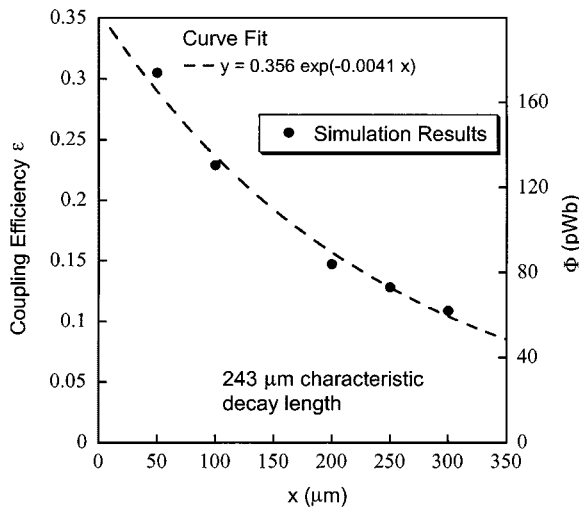


Fig. 4. Flux transmission coupling efficiency calculated by a one-dimensional micromagnetic simulation.

do learn that the flux coupling between the drive and pickup lines is not negligible in the DC limit.

B. Calculation of Self-Inductance

To prevent the Ni-Fe film from perturbing the write driver interconnects, the interconnect self-inductance when the film is in place must not be too large. The self-inductance can be calculated from the flux cutting through the film

$$\Phi = \frac{\mu H l \delta}{2} = LI \quad (2)$$

where L is the self-inductance. The relative permeability μ_r is given by [4]

$$\mu_r = \frac{M_s}{H_k + \frac{\pi M_s \delta}{4w}} \quad (3)$$

where M_s is the saturation magnetization of the film and H_k is the anisotropy. Combining (2) and (3) and making use of $H_P = I/2w$ yields

$$L = \frac{\mu_0 M_s l \delta}{4w H_k + \pi M_s \delta} \quad (4)$$

The substitution of $M_s = 800$ kA/m, $H_k = 400$ A/m, $\delta = 200$ nm, $w = 100$ μm , and $l = 8$ mm gives a Ni-Fe loaded self-inductance of $L = 2.4$ nH. This low value of self-inductance indicates low perturbation of the write driver interconnects, where the Ni-Fe slab is present over only one of the differential conductors.

C. System Bandwidth

The resonance frequency of the current probe can be calculated using simple ferromagnetic resonance theory [4]. Using the values given above in the equations

$$H_{k,DE} = \frac{\pi M_s \delta}{4w},$$

$$\omega = \mu_0 \gamma \sqrt{M_s (H_B + H_k + H_{k,DE})} \quad (5)$$

along with $H_B = 0$ A/m, $H_{k,DE} = 1.26$ kA/m, and making use of $\gamma = 2\pi \times 28$ GHz/T, we get approximately 1.3 GHz for the precessional frequency ω . However, the precessional frequency of the ferromagnetic element is not the system bandwidth. Frequency components greater than ω still have a sufficient SNR to permit the extraction of relevant data. Analysis of the spectral shape of the measured data reveals a bandwidth greater than 4 GHz, which indicates that the system is capable of measuring current rise times as short as 90 ps.

D. Linear Response and Deconvolution

To extract the actual pulse current waveform from the systems response to a pulse current requires a deconvolution of the measured system response with a measured impulse response. This operation is more easily performed in the frequency domain. After the subtraction is performed on the raw saturated and unsaturated system response data, the data are integrated to give the time-dependent induced flux. The impulse response data are also integrated to give the flux induced by the impulse.

Let us consider the inductive current probe as a “black box” linear system with input I (current) and output V (induced voltage) and with a system response function denoted as μ_{12} . The time domain expression $V_P = -d\Phi/dt$ corresponds to the frequency domain expression $V(\omega) = -i\omega\Phi(\omega)$. Also, we can make use of the fact that convolution in the time domain corresponds to multiplication in the frequency domain. The expression for flux in the frequency domain (signified by the tilde) is

$$\tilde{\Phi} = G\mu_0 \tilde{\mu}_{12} \tilde{I} \quad (6)$$

where G is a geometrical coupling factor that changes with conductor-to-conductor gap distance. This leads to

$$\tilde{V}_{\text{STEP}} = -i\omega G\mu_0 \tilde{\mu}_{12} \tilde{I}$$

$$\tilde{V}_{\text{IMPULSE}} = -i\omega G\mu_0 \tilde{\mu}_{12} I_0 \quad (7)$$

where we make use of the fact that the impulse function in the time domain is unity in the frequency domain. Note that the experimentally generated impulse is not a perfect value of unity;

thus the amplitude associated with the impulse is left unspecified as I_0 . We are then left with the deconvolved result in the frequency domain:

$$\frac{\tilde{V}_{\text{STEP}}}{\tilde{V}_{\text{IMPULSE}}} = \frac{\tilde{I}}{I_0}. \quad (8)$$

Care must be exercised with this result to avoid instability problems for frequencies where the denominator is small. The final time domain current waveform is obtained using the inverse Fourier transform.

IV. DISCUSSION

The data, as presented, were taken at a conductor spacing (as defined above) of 100 nm with no longitudinal bias field applied. We measured test structures fabricated with a larger conductor separation, but the 100 nm spacing gave the best SNR while still maintaining a conductor spacing large enough to minimize coupling with no Ni-Fe slab present.

It must be made very clear that no differential measurements are presented in this work; our equipment uses single-ended coaxial connections, and the outermost conductors shown in Figs. 1 and 2 are not used in any way. This work is, however, still applicable to differential write-driver interconnects because the Ni-Fe slab would be present over only one line in an actual differential interconnect used in a real drive measurement.

The coaxial microwave probes used must be pressed firmly against the stainless steel ground plane pads; otherwise the results obtained are unrepeatable. The actual repeatability of the measurement is usually quite good (better than 5%) when reasonable care is taken to make sure the Ni-Fe film lies flat on the surface of the current probe. Minor differences in film spacing, due to dust particles, appear as field strength variations (these are small variations in which the field strength continues to remain in the small signal regime) and signal pickup variations (which are removed by the background subtraction process applied to the saturated magnetic film).

It is important to verify that the Ni-Fe slab does not perturb the characteristic impedance of the write driver interconnects when the slab is in place. To do this, we performed transmission measurements on the drive line interconnects using a 10 V pulse with a 90 ps rise time. The results showed that the voltage perturbation with the slab in place was not significant and the rise time variation was less than 1 ps. We also performed transmission measurements using a 1 V, 100 ps wide impulse. The impulse amplitude was slightly reduced, about 5%, while the rise and fall times were not affected. This small amount of perturbation is to be expected, since the Ni-Fe slab is thin compared to the ground plane, and indicates that the current waveform measured is the same regardless of whether the slab is present or not.

Artifacts seen in the reconstruction of the input current pulse (precursor and oscillations) are due to the limited bandwidth associated with the deconvolution process. If a larger bandwidth is used, then division by zero becomes a problem with the denominator of (8). The precursor structure seen in Fig. 7 is not currently understood. The bandwidth of the measurement could be further improved if narrower conductors were used in the current probe test structure.

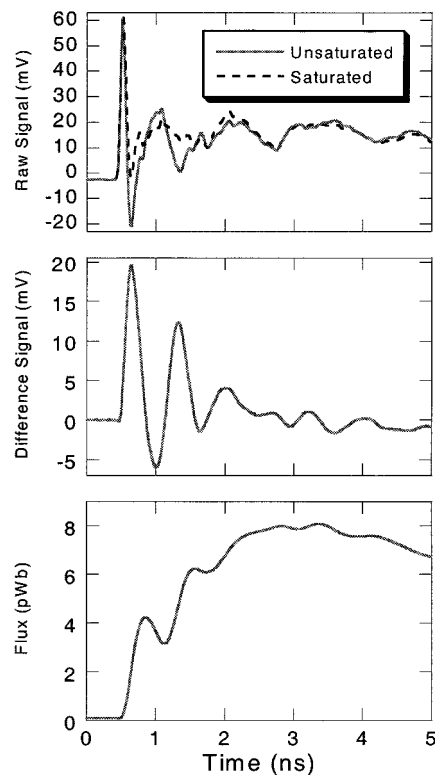


Fig. 5. Response of inductive current probe to current pulse. The top trace is the raw saturated and unsaturated signals. The middle trace is the difference of these two signals. The bottom trace is the result of integrating the difference signal.

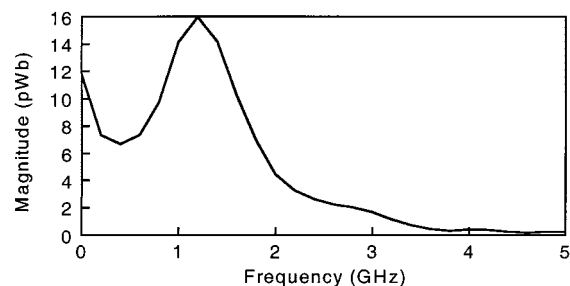


Fig. 6. Spectral response of pulse current waveform. Note resonance frequency around 1.2 GHz, however, spectral power is evident to 4 GHz.

V. RESULTS

Fig. 5 shows the response to the input current pulse obtained from the raw data acquired with the digital sampling oscilloscope. The top data set is the raw voltage waveforms taken with the Ni-Fe film in a magnetically saturated state, and with the film in a state where it is allowed to rotate freely. The middle set of data shows the difference signal obtained by subtracting the two raw datasets. The bottom trace shows the difference signal after integration. The sag seen at the end of this trace is due to the inductive nature of the technique. The lower cutoff frequency associated with this “high pass” response is about 20 MHz, deduced from the approximate sag time constant of about 8 ns.

The spectral response of the current probe to an applied current pulse is shown in Fig. 6. The resonance frequency shown is about 1.2 GHz. This is close to the value of 1.3 GHz predicted by theory. Note that there is considerable spectral power past

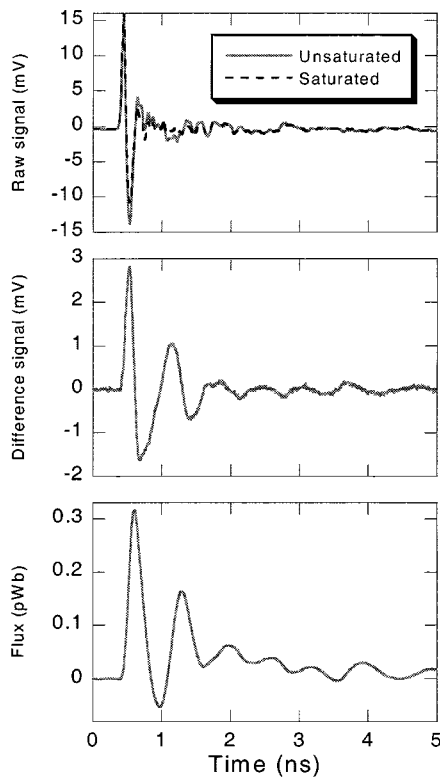


Fig. 7. Impulse response of inductive current probe. The top trace is the raw saturated and unsaturated signals. The middle trace is the subtracted difference signal. The bottom trace is the integrated difference signal.

the resonant peak; useful signal can be seen as far out as 4 GHz. Since this technique uses deconvolution of the system response to extract the relevant data, this additional bandwidth results in an improved switching response time.

Data from the system impulse response are shown in Fig. 7. The top, middle, and bottom traces show the raw impulse data, difference signal, and integrated result. The signals seen in the top of the figure are very similar, and it would seem difficult to obtain a meaningful difference; however, this technique has been used to extract useful difference signals from large raw signals: signals as small as 10 mV have been reproducibly extracted from 10 V raw signals. As indicated before, an oscilloscope with low drift, low noise, and large dynamic range is required. The integrated pulse current result obtained above is deconvolved (using the above frequency domain techniques) with the measured impulse response to obtain the step current waveform from the current probe.

Fig. 8 shows the spectral response of the probe system to a 1 V, 100 ps wide impulse. The resonant frequency is similar to that shown in Fig. 6, and there is clearly useable spectral power evident to 4 GHz.

Fig. 9 shows the final deconvolved step current waveform. The rise time t_R shown in the figure is 90 ps and the band-

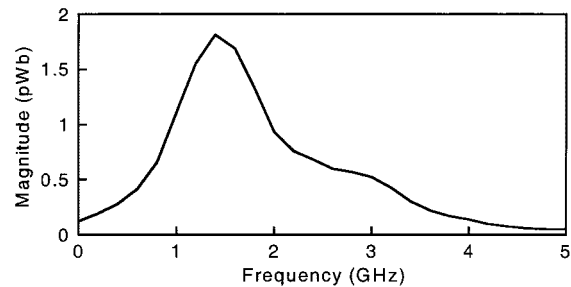


Fig. 8. Spectral response of impulse waveform. Resonance frequency is still around 1.2 GHz. Note spectral power evident to 4 GHz.

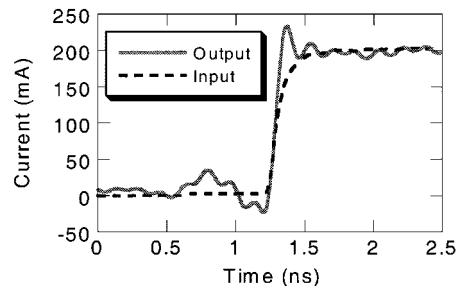


Fig. 9. Final current probe waveform. Also shown is the original fast current pulse sent into the drive side interconnects. Note precursor and oscillations due to finite bandwidth effects associated with the deconvolution process.

width of the measurement inferred from $BW = 0.35/t_R$ is about 3.9 GHz. Also shown in Fig. 9 is the voltage pulse, which was sent into the drive side interconnects, converted to current by dividing by 50 ohms. The current probe replicates this waveform reasonably well. Data taken at various longitudinal bias fields, from 80 A/m (1 Oe) to 8 kA/m (100 Oe), show a virtually identical current switching waveform, with only a noticeable increase in the noise level at higher bias fields due to decreased signal level. For simplified usage in disk drive applications, an external bias field is not required.

The inductive current probe is a useful tool for characterizing head field rise times and inferring the overall write channel bandwidth. The low cost, high bandwidth, and relative ease of implementation of the inductive technique makes it a useful tool for disk drive manufacturers.

REFERENCES

- [1] K. B. Klaassen and J. C. L. van Peppen, "Nanosecond and sub-nanosecond writing experiments," *IEEE Trans. Magn.*, vol. 35, pp. 625–631, Mar. 1999.
- [2] K. B. Klaassen, R. G. Hirko, and J. T. Contreras, "High speed magnetic recording," *IEEE Trans. Magn.*, vol. 34, pp. 1822–1827, July 1998.
- [3] T. J. Silva, C. S. Lee, T. M. Crawford, and C. T. Rogers, "Inductive measurement of ultrafast magnetization dynamics," *J. Appl. Phys.*, vol. 85, pp. 7849–7862, June 1999.
- [4] A. B. Kos, T. J. Silva, and P. Kabos, *Pulsed Inductive Microwave Magnetometer*. Unpublished.